Polypropylene nanocomposites reinforced with low weight percent graphene nanoplatelets

CrossMark

Adarsh Pradip Bafana [a, c], Xingru Yan [b], Xin Wei [a], Manisha Patel [a], Zhanhu Guo [b, *],
Suying Wei [c, **], Evan K. Wujcik [a, ***]

[a] *Materials Engineering And Nanosensor (MEAN) Laboratory, Dan F. Smith Department of Chemical Engineering, Lamar University, Beaumont, TX, 77710, USA*
[b] *Integrated Composites Laboratory (ICL), Department of Chemical and Biomolecular Engineering, University of Tennessee, Knoxville, TN, 37996, USA*
[c] *Department of Chemistry and Biochemistry, Lamar University, Beaumont, TX, 77710, USA*

ARTICLE INFO

ABSTRACT

Polypropylene (PP) based graphene nanocomposites (NCs) find diverse applications in material science such as a material for making lightweight storage tanks. Herein, NCs with graphene nanoparticles (GnPs) and PP were prepared, using solution mixing method. GnPs have a slight effect on the crystalline structure of PP, as shown by X ray diffraction (XRD) results; thereby rendering the functionality of PP intact. There were little changes in the rheological behavior of the composite and the frictional losses incurred due to mobility of polymer chains were reduced with an increase in the GnP loading from 0.5% to 5%—a range not yet explored.

© 2016 Elsevier Ltd. All rights reserved.

1. Introduction

Nanocomposites are materials which have at least one of the phases that show dimensions in the nanometer scale [1]. These are high performance materials which find diverse applications in industry ranging from packaging [1] to automobiles [2]. Okada et al. [3] from Toyota research group was the first who prepared commercial polymer nanocomposites (PnCs) by solution polymerization of caprolactam in the clay galleries for nylon composites [4].

PnCs are hybrid materials, in which mixing of the filler phase is achieved at the nanometer level, so that at least one dimension of the filler phase is less than 100 nm [5]. During recent years, these nanocomposites have generated much research interest owing to remarkable enhancements in the various composite properties at very low volume fractions [6]. One such PnC with filler material polypropylene and graphene nanoplatelets is elaborately studied in this paper. Graphene, a monolayer of sp²-hybridized carbon atoms arranged in a two-dimensional honeycomb lattice, has attracted

tremendous attention in recent years owing to its exceptional thermal, mechanical, and electrical properties [7–10] The applications of graphene include but are not limited to field effect transistors (FET), sensors, transparent conductive films, clean energy devices and graphene polymer nanocomposites [10,11].

One of the most promising applications of this material is in polymer nanocomposites [6], wherein PnCs of graphene in various polymers such as polypropylene (PP) and polyethylene (PE) have been made [7,12,13] Mohammad et al. [14] reported the enhanced fracture and fatigue properties of graphene based epoxy nanocomposite as compared to CNT nanocomposite. Ramanathan et al. [15] reported an unprecedented shift in glass transition temperature of over 40 °C was obtained for poly(acrylonitrile) at 1 wt% functionalized graphene sheet, and with only 0.05 wt% functionalized graphene sheet in poly(methyl methacrylate) there was an improvement of nearly 30 °C. Modulus, ultimate strength and thermal stability follow a similar trend, with values for functionalized graphene sheet– poly(methyl methacrylate) rivalled those for single-walled carbon nanotube–poly(methyl methacrylate) composites [15]. TiO₂- graphene nanocomposites also opened up new ways to obtain photoactive graphene-semiconductor composites [16].

The unparalleled advantages of these PnCs include cost-effective processability, light weight, and tunable mechanical, magnetic and

---

* Corresponding author.
** Corresponding author.
*** Corresponding author.
   E-mail addresses: zhanhu.guo@lamar.edu (Z. Guo), suying.wei@lamar.edu (S. Wei), Evan.Wujcik@lamar.edu (E.K. Wujcik).

electrical properties make these materials favourable in versatile applications [17,18]. Today, PP finds significant use as a polymeric matrix for polymeric composites and nanocomposites. Wambua et al. [19] in their work synthesized polymeric composite of PP and a natural fiber-kenaf. The results indicated high specific properties and presented an excellent potential for utilization in reinforcement of plastics while still containing a substantial amount of renewable materials in them [19].

Roes et al. [20] conducted a study on the cost and environmental impact of PP as a material for making nanocomposites. Based on the Life cycle analysis (LCA) and Life cycle costing (LCC), they concluded that the use of PP nanocomposites only have advantages over other polymeric alternatives such as low density polyethylene (LDPE), without causing much harm to the environment [20]. This is due to the fact that lower amount of material is needed for the same purpose while using PP because of its better mechanical properties such as Young's modulus and tensile strength [20]. All this and articles on development of PP based nanocomposites made PP based composites with nanofillers quite popular and we thus found it suitable for synthesis of our nanocomposite.

In the present work, PP/graphene nanocomposites (NCs) with graphene filler have been made in the loading range of 0.5–5 wt. %. The aim of this work is to study the effect of graphene on physical, mechanical, and morphological properties of polypropylene. The loading in the range of 0.5–5 wt % has only recently been explored [21] and studying the effects of the PnC at such a low loading range adds to the novelty of this work owing to its relative nascent exploration due to paucity of work done in this loading range.

2. Materials and methods

2.1. Materials

Polypropylene (PP) was supplied by Total Petrochemicals, Inc USA. Xylene (laboratory grade, $\rho = 0.87$ g/cm^3) was purchased from Fisher Scientific Inc. Graphene was purchased from Angstron Materials having a product code N008-P-40, with its true density being ≤ 2.20 g/cm^3 and an oxygen content of $\leq 1.00\%$ (by weight). All the chemicals were used as-received without any further treatments.

2.2. Synthesis methods

The PP/graphene nanocomposites with 0.5, 1.5, 2.5, 5 wt% graphene were prepared. For 5% PP/graphene nanocomposite- 1.039 g of graphene and 19.759 g of PP was dissipated into 200 ml of Xylene and magnetically stirred at 140 °C for 2 h, in order to allow the PP to dissolve completely. After 2h graphene powder was added and ultrasonication (30 min) were subsequently performed to disperse the NGPs in the PP solution and then magnetically stirred for more 2h. Finally, the PP/graphene nanocomposites were removed from cooling the solution using deionized ice water. After that the PNCs were dried in a vacuum oven at 60 °C for 48 h to eliminate the residue DI water. These PP/graphene nanocomposites were hot pressed in a circular/cylindrical shape, 15 samples were made at 180 °C for conducting different experiment and tests.

The synthesis of PnCs was done using solution mixing as solution mixing has been widely used as an effective technique for fabrication of graphene/PNCs, because of the ease of processing graphene and its derivatives in water or organic solvents [22,23].

2.3. Characterization methods

The morphologies of pure PP and GnP/PP PnCs were characterized using a JEOL JSM-6510LV scanning electron microscope (SEM). The SEM specimens were prepared by coating with carbon.

The crystalline structure of pure PP and its Graphene/PP NPCs was studied by X-ray diffraction (XRD) analysis, which was carried out by a Bruker AXS D8 Discover diffractometer operating with a Cu Kα radiation source. The X-ray was generated at 40 kV and 27 mA power and XRD scans were recorded at 2θ from 5 to 80° ($\lambda = 0.154$ nm).

The thermal stability of the pure PP and Graphene/PP nanocomposites was investigated by thermogravimetric analysis (TGA, TGA-Q500 instrument). The heating rate was 10 °C min^{-1}, and the experiments were performed in a continuous air flow at a flow rate of 20 °C min^{-1}. The temperature was in the range 25–700 °C. The effects of the nanoparticles on the thermal properties of the polymer in the polymer nanocomposites were determined by using differential scanning calorimetry (DSC). Heating scans were performed at a rate of 10 °C min^{-1} in a continuous nitrogen flow at a rate of 20 cm^3 min^{-1}. The samples were sealed in a standard aluminium pan. The measurements were completed in the temperature range 25–250 °C. The weight of each sample was approximately 10 mg. The DSC heat flow and temperature values were calibrated with an indium standard.

Melt rheological properties of Neat PP and its PNCs were investigated by TA Instruments AR 2000ex Rheometer. The frequency sweep was from 100 to 0.1 Hz. An environmental test chamber (ETC) steel parallel-plate geometry was used to perform the measurement at 230 °C in linear viscoelastic (LVE) range with strain 1% under air atmosphere.

Dynamic mechanical analysis (DMA) was studied by a TA Instruments AR 2000ex machine in torsion rectangular mode with a strain 0.4% and a frequency of 1 Hz in the temperature range of 30–140 °C.

3. Results and discussion

3.1. Thermal stability

Thermal stability is a vital factor for characterization of a polymeric material as most frequently it is the temperature that puts a check on the possible utilization of a material. Owing to the sheet like structure of graphene, it had effects on the thermal properties of the nanocomposite substantial enough to examine them. This section provides the results of Thermogravimetric Analysis (TGA) and Differential Scanning Calorimetry (DSC).

The thermal stability of pure PP and PNCs of PP with various fractions of graphene was tested using TGA. Weight fractions of 0.5, 1.5, 2.5 and 5% graphene with PP was tested.

The two graphs in Fig. 1(A) and (B) are the TGA weight loss curve and the derivative weight loss curves of pure PP, graphene and PP/graphene PnCs, respectively.

In the weight loss curve it was shown that the thermal stability of pure PP was lower than that of the graphene/PP PnCs. There was also an increase in stability with an increase in the weight fractions of graphene in the PnCs.

Table 1 shows the discrete values of temperatures at the onset of degradation (T_i), at 10% degradation ($T_{10\%}$) and at the maximum thermal degradation (T_{max}) of the various GnP loadings.

It was clearly evident that each of the degradation temperatures increased with an increase in the fraction of graphene in the PnC. However, this increase in the degradation temperature was not linearly proportional. For instance, the change in T_i from pure PP to 0.5 wt % graphene loaded PP was 2 °C while that for increase from 0.5% to 1.5% was 14 °C, for increase from 1.5% to 2.5% was 5 °C and finally for 2.5%–5% was 45 °C. This shows an increase in the onset degradation temperature by 66 °C for 5 wt% graphene PnC as compared to pure PP.
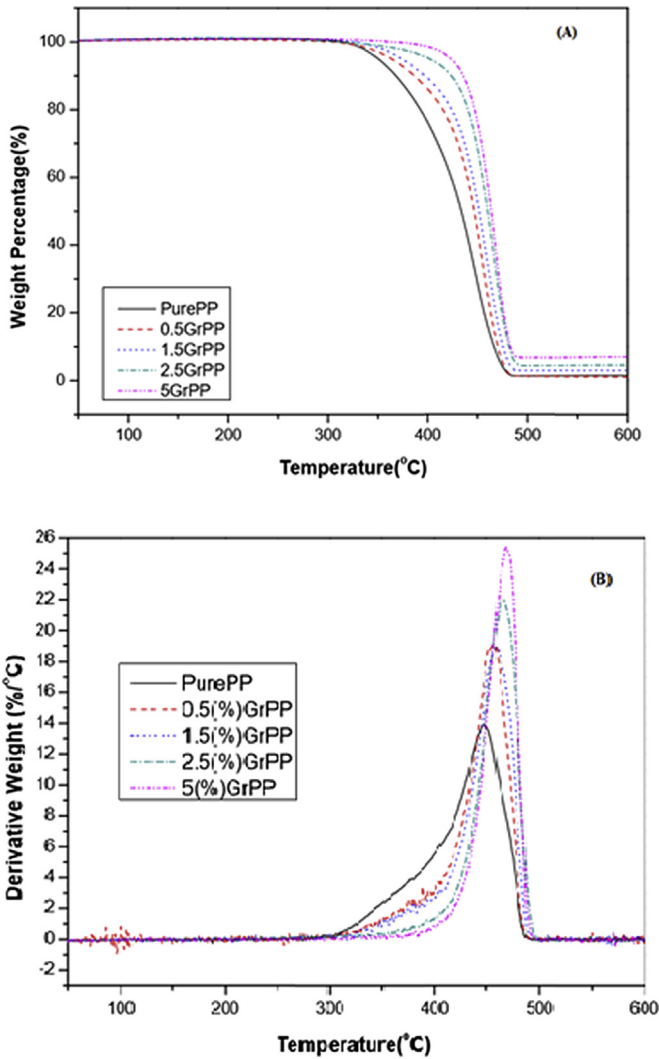
Similar increase in degradation temperatures were noted by

Fig. 2. DSC thermograms of PP/graphene nanocomposites with different graphene loadings.

slightly compared to that of PP (see Table 2) [18]. The degree of crystallinity was calculated using equation (1),

$$D = \frac{\Delta H_m}{\Delta H_0 \, f_{PP}} \times 100\% \tag{1}$$

Where D is the degree of crystallinity, H_m is the melting enthalpy, ΔH_0 is the melting enthalpy of the 100% crystalline PP, which is reported to be 209 J g^{-1}, and f_{pp} is the PP weight fraction in the composites [18,24].

3.2. Morphological analyses

These are used to study the characteristics related to the morphology or structure of the PNC. The studies on morphological analyses done in the current work were to study the porosity of the material as well as the nanocomposite's crystalline structure.

Fig. 3 shows the X-ray diffraction (XRD) patterns of the neat PP and PP/graphene PNCs with different weight percentages. Isotactic polypropylene displays remarkable complexity in its crystal structure [25]. The α phase is most prevalent though there is the presence of a β phase as well [24,25]. This complexity of structure led to the subsequent explanation of the XRD analysis.

In Fig. 5 above, the peak at around $2\theta = 26.07°$ corresponds to the graphene nanoplatelets. The diffraction peaks at $2\theta = 14.2, 17, 18.8$ and $20°$ correspond to (110), (040), (130) and (111) planes of α crystal of PP, respectively, while the overlapping peaks between 21.1 and 22.1°, were attributed to a combination of α-phase (131 and 041) and β-phase (301) of PP. The small peak at 25.4° corresponded to α − form PP (060) [17]. According to the Scherrer Equation (2) gives the average crystallite size can be estimated by XRD pattern [17],

Fig. 1. **(A)** TGA weight loss curves and **(B)** derivative weight loss curves of pure PP and PP/graphene PNCs.

Table 1
TGA data of the pure PP and graphene Nanocomposites. T_i: Temperature of onset degradation; T 10%: Temperature of 10% mass loss, T_{max}: Inflection point.

GnPsloading (wt %)	PurePP(0)	0.5	1.5	2.5	5
T_i [°C]	327	329	343	348	393
$T_{10\%}$ [°C]	368	386	397	423	435
T_{max} [°C]	447	456	461	468	471

Achaby et al. [7]. They pointed out that the increase in thermal stability with addition of graphene to form a PNC could be attributed to the hindered diffusion of volatile decomposition products within the nanocomposites, which in turn was highly dependent upon the nanoparticle-polymer chain interactions.

In addition, it had also been discussed in literature that thermal oxidative degradation of PP should be studied as it is under an atmosphere of air that most polymeric materials re commonly used [17]. With this observation in mind, TGA was carried out in an atmosphere constituting of air-nitrogen mixture.

Fig. 2 compares the non-isothermal crystallization curves as measured by DSC. GnPs had a small effect on the melting temperature and increased the onset meting temperature (T_m) only
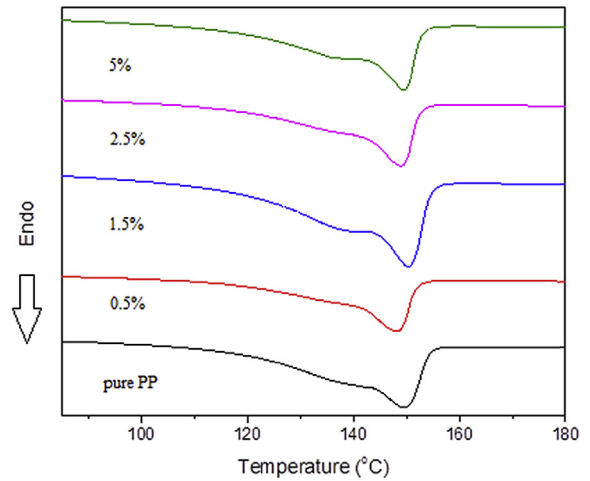
Table 2
DSC data of pure PP and PP/Graphene nanocomposites. T_{on}: onset melting temperature; T_m: melting temperature; ΔH_m: melting enthalpy; D: degree of crystallinity; ΔD: variation in the degree of crystallinity.

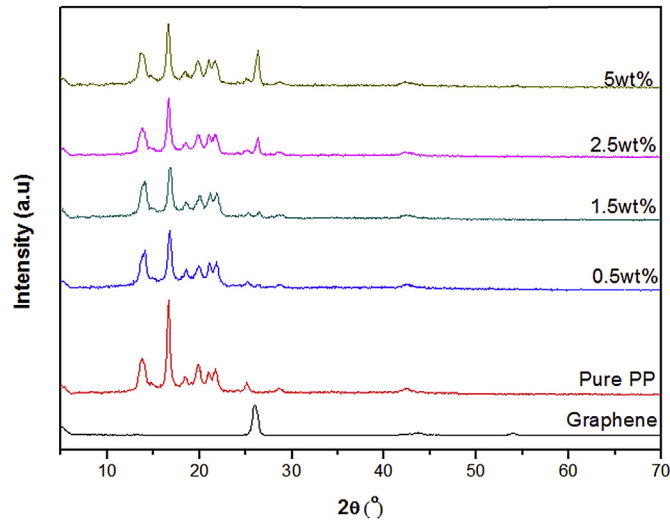| GnP loading (wt %)	T_{on} (°C)	T_m (°C)	H_m (J.g^{-1})	D (%)	ΔD (%)
0	135.26	149.62	77.41	37.03	—
0.5	136.93	148.26	65.48	31.48	7.08
1.5	138.35	150.18	74.4	36.14	0.89
2.5	137.96	148.9	69.23	33.97	6.14
5	138.31	149.5	72.31	36.41	0.6

Fig. 3. X-ray diffraction (XRD) patterns of the neat PP and PP/graphene PNCs.

$$L = \frac{k\lambda}{\beta \cos \theta} \tag{2}$$

where L is the average crystallite size, k is the shape factor, λ is the wavelength ($\lambda = 0.154$), β is the full width at half maximum, and θ is the angle at maximum intensity. The value of k depends on several factors, including the miller index of the reflection plane and the shape of the crystal, which is normally 0.89 if the shape is unknown.

Shown in Fig. 4, the GnPs are separated from each other in the PNCs with a GnP loading of 1.5 wt%. SEM is used to characterize the morphology of our sample. Fig. 6 shows the SEM of a 1.5 wt % sample of the PP/graphene nanocomposite. The SEM displayed well dispersed graphene onto the polymer matrix. This helped us infer that the graphene was well bound onto the polymeric matrix [24]. According to Stankovich et al. [26], the quality of nanofiller dispersion in the polymer matrix directly correlates with its effectiveness for improving its properties; thus they carried out SEM the high aspect ratio sheet images of which led to the conclusion that it showed great potential. A similar case of obtained in the present work.

3.3. Melt rheological properties

Rheological properties of materials are important because the choice of material form and physical state is more than a matter of convenience: product performance issues are usually related to solid sample properties; process ability issues can be correlated

with polymer melt properties [27]. Besides, graphene's strong structural and mechanical properties make it vital to understand its effects on the PnC [8]. Defect-free graphene is the stiffest material (E ~ 1 TPa) ever reported in nature and also has superior intrinsic strength, ~130 GPa [8,28]. Despite some structural distortion, the measured elastic modulus of CRG sheets is still as high as 0.25 TPa [8,29]. Advantages of graphene in mechanical reinforcement over existing carbon fillers such as CB, EG, and SWCNT have also been discussed [8,30–32]. The above stated discussion provided for the motivation to study the rheological and mechanical properties of the PnCs.

Rheoogical tests can be measured as the material undergoes temperature induced changes from amorphous to crystalline; solid to molten and vice versa. Rheological tests on thermoplastic melts measure a material's flow properties and provide vital information about polymer processing.

The storage and loss moduli of PP and its nanocomposite melts with GnP filler loading of 0.5, 1.5, 2.5 and 5 wt% at 200 °C are presented in Fig. 7 (A and B), with a log-log plot as a function of angular frequency (ω). Fig. 5(C) shows the mechanical loss factor (tan δ) of PP/GnP nanocomposites with different GnP loading.

The following equations help to understand the viscoelastic behavior of the composite:

$$G' = \left(\frac{stress}{strain}\right) cos\theta \tag{3}$$

$$G'' = \left(\frac{stress}{strain}\right) sin\theta \tag{4}$$

$$tan\delta = \frac{G''}{G'} \tag{5}$$

where, G' is the storage modulus and represents the measure of elasticity of the material. G'' is the loss modulus representing the energy lost or dissipated as heat due to the effects of stress. tan δ is a measure of the material damping. In other words, G' represents the elastic region of the material whereas G'' shows the viscous region of the material and tan δ gives a measure of the viscous portion to the elastic portion.

From the plots it was deduced that the storage and loss moduli of the PNCs decreased with an increase in the angular frequency. The mechanical loss property (tan δ) which is the ratio of loss modulus (G'') to storage modulus (G') is related significantly to the applied ω. The tan δ value increases with an increase in the value of ω and this accounts for the solid like behavior of the PNC. Another aspect noticed on increasing the values of ω is that the tan δ of the PNC melt shows three different stages: rubbery, viscoelastic and glassy state, consistent with findings reported [27].
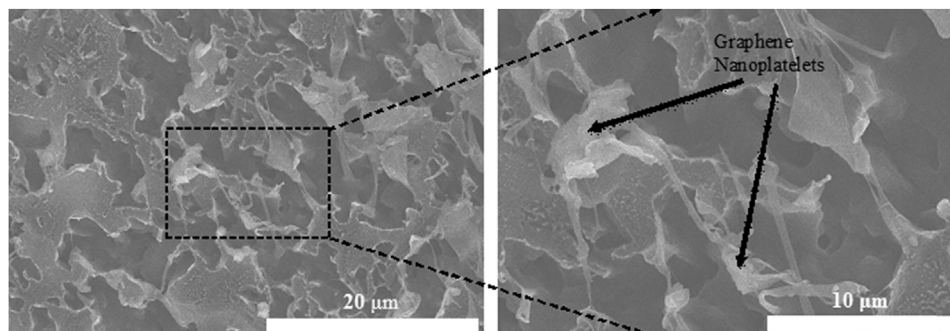

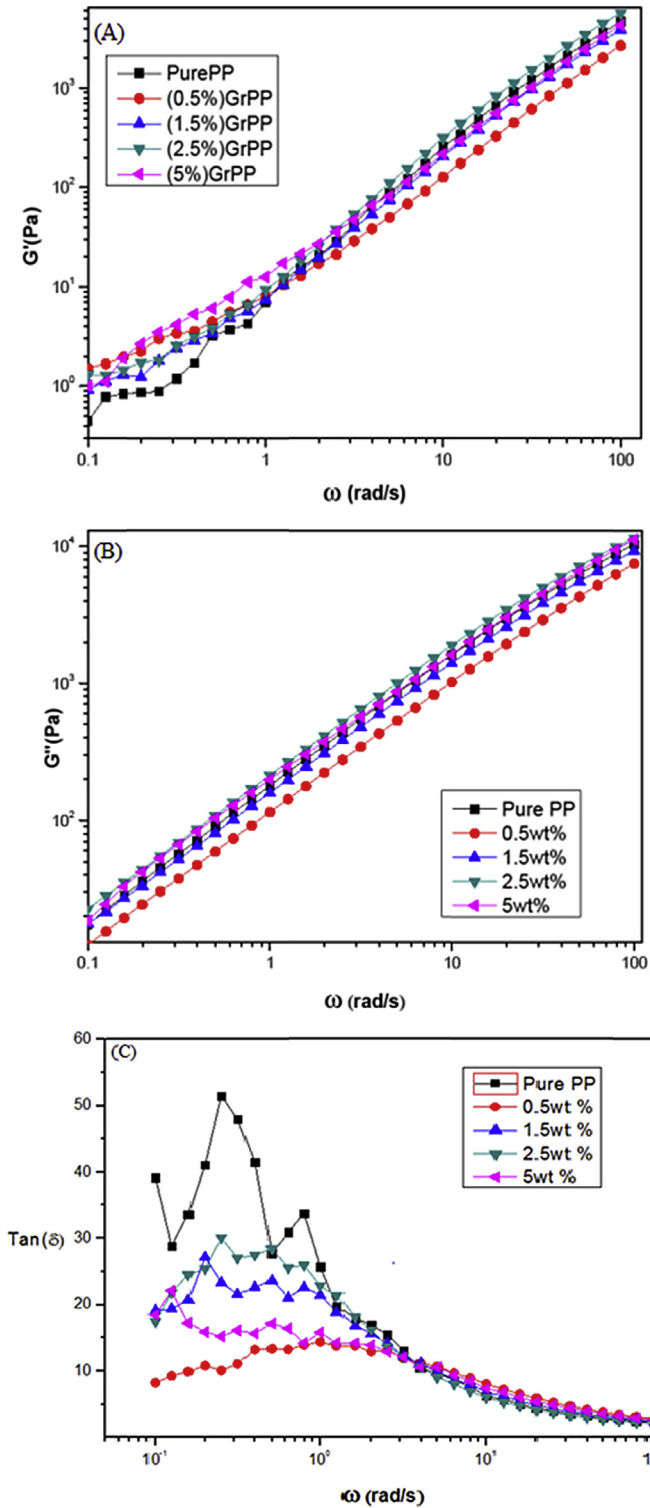**Fig. 4.** SEM images of PP PNCs with graphene nanoplatelet loading of 0.5 wt %.

Fig. 5. **(A)** storage modulus (G′), **(B)** loss modulus (G″), **(C)** mechanical loss factor (tan δ) for PP and its PNCs.

Fig. 6. **(A)** Storage Modulus (E′) and **(B)** loss modulus (E″) vs. temperature for the pure PP and nanocomposites with different graphene nanoparticle loadings.

Fig. 7. Viscosity v/s shear rate for GnP/PP PnCs.

In addition to the above measurements, tests were done to study the effect of frequency or shear rate on the viscosity as it can be used to study the dispersion of GnPs in the PP matrix [7,33–35].

Pure PP and GnP/PP PnCs were studied for the frequency range from 10^{-2} to $10 \, s^{-1}$. The viscosity shows an increase at low values of shear rates and decreases with an increase in the shear rate as shown in Fig. 7. The increase in viscosity at low shear rates implying
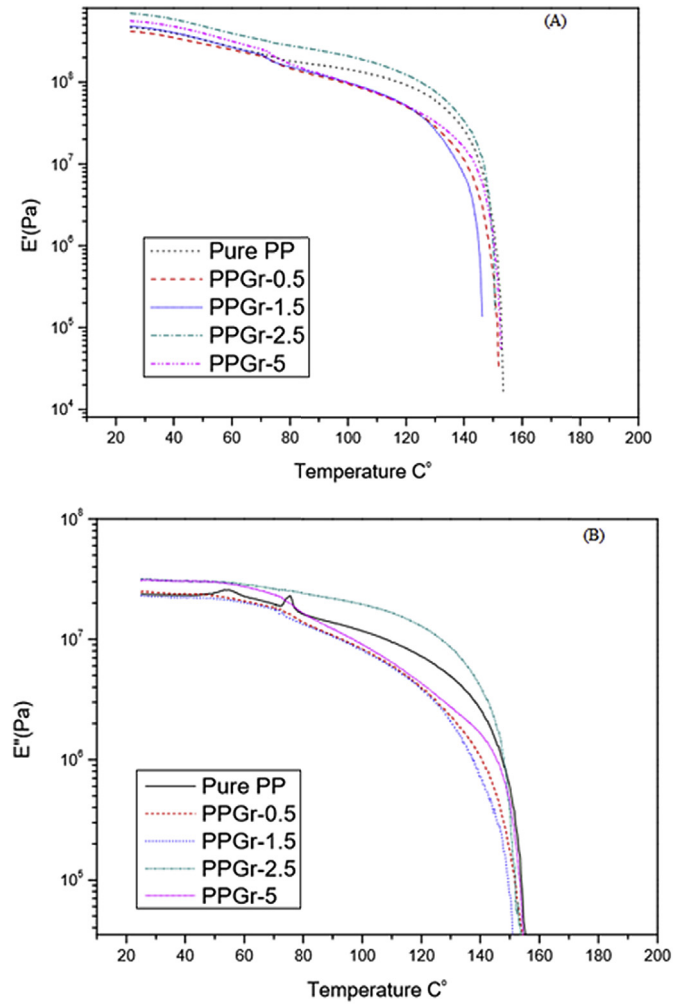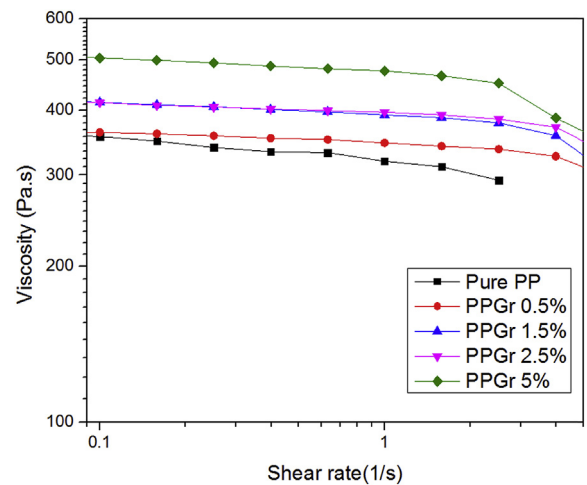
good dispersion of GnPs in the PP matrix, which is in agreement with results obtained from literature [7,33–35]. The threshold effect shows distinctly somewhere in between 2.5% and 5%(by weight) of GnP loading and the decrease in viscosity with

increasing shear rate is due to the shear thinning behavior of the PnC, which is concomitant to the findings in literature [34].

3.4. Dynamic mechanical analysis (DMA)

Dynamic mechanical analysis (DMA) is used to characterize the viscoelastic properties of the materials by providing specific information on the storage modulus (E′), loss modulus (E″) and tan δ within the investigated temperature range [17]. The storage modulus gives the elastic modulus of the nanocomposite while the loss modulus is a measure of the frictional losses incurred (energy dissipated) due to the motion of polymer chains. The change in E′ with temperature is shown in Fig. 6 (A). It shows that with increasing the amount of the GnP loading the value of E′ decreases slightly with temperature. This trend agrees well with that of Young's modulus due to the plasticization effect of low modulus of PP latex [7]. The magnitude of increase of storage modulus is lower than that of Young's modulus, which may be due to the difference of the measurement modes and the resolution of instruments. A similar observation is made even in case of change in loss modulus with temperature, as shown in Fig. 6 (B). A decrease in loss modulus with increasing GnP loading across a temperature range implied that GnPs brought about a decrease in the frictional losses due to the motion of polymer chains. These observations help us to conclude that increasing loading of GnPs into the PP matrix aids in reducing the frictional losses in the composite thereby increasing Section Headings.

4. Conclusions

In the present work a PP/graphene nanocomposite was prepared and a thorough thermal, mechanical, and morphological characterization of the same was carried out. The nanocomposite of PP/graphene finds immense utility as material for preparation of light weight automotive vehicle and graphene finds application as in a PP based nanocomposite due to the ease with which it can be processed and the enhancement it brings about in PP without altering its composition starkly. This enhancement without much deviation in the properties of pure PP that addition of GnP gets to the nanocomposite make it an attractive alternative to other nanomaterials which may be used for production of polymer based nanocomposites.

The characterization studies led to conclusions which affirm the use of PP based graphene nanocomposites. Thermal analyses using TGA showed improved stability of the PNC with increased graphene loading while the results of DSC clearly helped to conclude that increased graphene loading led to an increase in the onset temperature at which degradation begins. Through the mechanical analysis it could be deduced that the frictional losses that occur due to motion of polymer chains were reduced with addition of GnP. The inferences from morphological tests were also pretty motivating. XRD studies revealed the presence of graphene in the PNC and the presence did not affect the crystalline structure of the PP matrix thereby leading to the conclusion that the GnP do not cause much transformation in the physical structure of the polymer matrix and can hence be confidently used as a filler material for polymer nanocomposites.

Acknowledgements

References

[1] Anandhan S, Bandyopadhyay S. Polymer nanocomposites: from synthesis to applications. INTECH Open Access Publ 2011. http://cdn.intechopen.com/pdfs/17184/InTech-Polymer_nanocomposites_from_synthesis_to_applications.pdf [accessed 28.03.16.].

[2] Hussain F, Hojjati M, Okamoto M, Gorga RE. Review article: polymer-matrix nanocomposites, processing, manufacturing, and application: an overview. J Compos Mater 2006;40:1511–75. http://dx.doi.org/10.1177/0021998306067321.

[3] Okada A, Fukushima Y, Kawasumi M, Inagaki S, Usuki A, Sugiyama S, et al. Composite material and process for manufacturing same. US4739007 A. 1988. http://www.google.com/patents/US4739007 [accessed 21.04.16.].

[4] Ramesh neppalli. Study on structure and morphology of polymer nanocomposites. 2012. http://paduaresearch.cab.unipd.it/4493/ [accessed 21.04.16.].

[5] Thomas S, Stephen R. Rubber nanocomposites: preparation, properties and applications. John Wiley & Sons; 2010.

[6] Potts JR, Dreyer DR, Bielawski CW, Ruoff RS. Graphene-based polymer nanocomposites. Polymer 2011;52:5–25. http://dx.doi.org/10.1016/j.polymer.2010.11.042.

[7] El Achaby M, Arrakhiz F-E, Vaudreuil S, el Kacem Qaiss A, Bousmina M, Fassi-Fehri O. Mechanical, thermal, and rheological properties of graphene-based polypropylene nanocomposites prepared by melt mixing. Polym Compos 2012;33:733–44. http://dx.doi.org/10.1002/pc.22198.

[8] Kim H, Abdala AA, Macosko CW. Graphene/Polymer nanocomposites. Macromolecules 2010;43:6515–30. http://dx.doi.org/10.1021/ma100572e.

[9] A. Geim, K. Novoselov, Collect Rev Nat J, [n.d.].

[10] Zhu Y, Murali S, Cai W, Li X, Suk JW, Potts JR, et al. Synthesis, properties, and applications. Adv Mater 2010;22:3906–24. http://dx.doi.org/10.1002/adma.201001068.

[11] Huang X, Yin Z, Wu S, Qi X, He Q, Zhang Q, et al. Graphene-based materials: synthesis, characterization, properties, and applications. Small 2011;7:1876–902. http://dx.doi.org/10.1002/smll.201002009.

[12] Wakabayashi K, Pierre C, Dikin DA, Ruoff RS, Ramanathan T, Brinson LC, et al. Polymer–graphite nanocomposites: effective dispersion and major property enhancement via solid-state shear pulverization. Macromolecules 2008;41:1905–8. http://dx.doi.org/10.1021/ma071687b.

[13] Kalaitzidou K, Fukushima H, Drzal LT. A new compounding method for exfoliated graphite–polypropylene nanocomposites with enhanced flexural properties and lower percolation threshold. Compos Sci Technol 2007;67:2045–51. http://dx.doi.org/10.1016/j.compscitech.2006.11.014.

[14] Rafiee MA, Rafiee J, Srivastava I, Wang Z, Song H, Yu Z-Z, et al. Fracture and fatigue in graphene nanocomposites. Small 2010;6:179–83. http://dx.doi.org/10.1002/smll.200901480.

[15] Ramanathan T, Abdala AA, Stankovich S, Dikin DA, Herrera-Alonso M, Piner RD, et al. Functionalized graphene sheets for polymer nanocomposites. Nat Nano 2008;3:327–31. http://dx.doi.org/10.1038/nnano.2008.96.

[16] Williams G, Seger B, Kamat PV. TiO$_2$-graphene nanocomposites. Uv-assisted photocatalytic reduction of graphene oxide. ACS Nano 2008;2:1487–91. http://dx.doi.org/10.1021/nn800251f.

[17] Song P, Cao Z, Cai Y, Zhao L, Fang Z, Fu S. Fabrication of exfoliated graphene-based polypropylene nanocomposites with enhanced mechanical and thermal properties. Polymer 2011;52:4001–10. http://dx.doi.org/10.1016/j.polymer.2011.06.045.

[18] Foresta T, Piccarolo S, Goldbeck-Wood G. Competition between α and γ phases in isotactic polypropylene: effects of ethylene content and nucleating agents at different cooling rates. Polymer 2001;42:1167–76. http://dx.doi.org/10.1016/S0032-3861(00)00404-3.

[19] Wambua P, Ivens J, Verpoest I. In: Some mechanical properties of kenaf/polypropylene composites prepared using a film stacking technique, in: 13th International Conference on Composite Materials Conference Proceedings. Beijing, China: The Chinese Society for Composite Materials and China Universities Alumni Association; 2001. p. 25–9.. In: http://iccm-central.org/Proceedings/ICCM13proceedings/SITE/PAPERS/Paper-1125.pdf [accessed 22.04.16.].

[20] Roes AL, Marsili E, Nieuwlaar E, Patel MK. Environmental and cost assessment of a polypropylene nanocomposite. J Polym Environ 2007;15:212–26. http://dx.doi.org/10.1007/s10924-007-0064-5.

[21] Galindo B, Benedito A, Gimenez E, Compañ V. Comparative study between the microwave heating efficiency of carbon nanotubes versus multilayer graphene in polypropylene nanocomposites. Compos Part B Eng 2016;98:330–8. http://dx.doi.org/10.1016/j.compositesb.2016.04.082.

[22] Cui Y, Kundalwal SI, Kumar S. Gas barrier performance of graphene/polymer nanocomposites. Carbon 2016;98:313–33. http://dx.doi.org/10.1016/j.carbon.2015.11.018.

[23] Yang J, Tian M, Jia Q-X, Shi J-H, Zhang L-Q, Lim S-H, et al. Improved mechanical and functional properties of elastomer/graphite nanocomposites prepared by latex compounding. Acta Mater 2007;55:6372–82. http://dx.doi.org/10.1016/j.actamat.2007.07.043.

[24] Li Y, Zhu J, Wei S, Ryu J, Sun L, Guo Z. Poly(propylene)/graphene nanoplatelet nanocomposites: melt rheological behavior and thermal, electrical, and electronic properties. Macromol Chem Phys 2011;212:1951–9. http://dx.doi.org/10.1002/macp.201100263.

[25] Cho K, Saheb DN, Choi J, Yang H. Real time in situ X-ray diffraction studies on the melting memory effect in the crystallization of β-isotactic polypropylene. Polymer 2002;43:1407–16. http://dx.doi.org/10.1016/S0032-3861(01)00729-7.

[26] Stankovich S, Dikin DA, Dommett GHB, Kohlhaas KM, Zimney EJ, Stach EA, et al. Graphene-based composite materials. Nature 2006;442:282–6. http://dx.doi.org/10.1038/nature04969.

[27] Magnetic polystyrene nanocomposites reinforced with magnetite nanoparticles - yan. 2013. Macromolecular materials and engineering - Wiley Online Library, (n.d.), http://onlinelibrary.wiley.com/doi/10.1002/mame.201300208/abstract;jsessionid=797730727F017FE11D1F4BF00305731D.f04t04?userIsAuthenticated=false&deniedAccessCustomisedMessage= [accessed 28.03.16.].

[28] Lee C, Wei X, Kysar JW, Hone J. Measurement of the elastic properties and intrinsic strength of monolayer graphene. Science 2008;321:385–8. http://dx.doi.org/10.1126/science.1157996.

[29] Gómez-Navarro C, Burghard M, Kern K. Elastic properties of chemically derived single graphene sheets. Nano Lett 2008;8:2045–9. http://dx.doi.org/10.1021/nl801384y.

[30] Steurer P, Wissert R, Thomann R, Mülhaupt R. Functionalized graphenes and thermoplastic nanocomposites based upon expanded graphite oxide. Macromol Rapid Commun 2009;30:316–27. http://dx.doi.org/10.1002/marc.200800754.

[31] Rafiee MA, Rafiee J, Wang Z, Song H, Yu Z-Z, Koratkar N. Enhanced mechanical properties of nanocomposites at low graphene content. ACS Nano 2009;3:3884–90. http://dx.doi.org/10.1021/nn9010472.

[32] Ramanathan T, Abdala AA, Stankovich S, Dikin DA, Herrera-Alonso M, Piner RD, et al. Functionalized graphene sheets for polymer nanocomposites. Nat Nano 2008;3:327–31. http://dx.doi.org/10.1038/nnano.2008.96.

[33] McNally T, Pötschke P, Halley P, Murphy M, Martin D, Bell SEJ, et al. Polyethylene multiwalled carbon nanotube composites. Polymer 2005;46:8222–32. http://dx.doi.org/10.1016/j.polymer.2005.06.094.

[34] Martin-Gallego M, Bernal MM, Hernandez M, Verdejo R, Lopez-Manchado MA. Comparison of filler percolation and mechanical properties in graphene and carbon nanotubes filled epoxy nanocomposites. Eur Polym J 2013;49:1347–53. http://dx.doi.org/10.1016/j.eurpolymj.2013.02.033.

[35] Zhang H-B, Zheng W-G, Yan Q, Jiang Z-G, Yu Z-Z. The effect of surface chemistry of graphene on rheological and electrical properties of polymethylmethacrylate composites. Carbon 2012;50:5117–25. http://dx.doi.org/10.1016/j.carbon.2012.06.052.